



**HAL**  
open science

## Observational evidence for active dust storms on Titan at equinox

S. Rodriguez, Stéphane Le Mouélic, J. Barnes, J. Kok, S. Rafkin, R. Lorenz,  
B. Charnay, J. Radebaugh, C. Nartea, T. Cornet, et al.

► **To cite this version:**

S. Rodriguez, Stéphane Le Mouélic, J. Barnes, J. Kok, S. Rafkin, et al.. Observational evidence for active dust storms on Titan at equinox. *Nature Geoscience*, 2018, 11 (10), pp.727-732. 10.1038/s41561-018-0233-2 . hal-02373155

**HAL Id: hal-02373155**

**<https://hal.science/hal-02373155>**

Submitted on 26 Oct 2023

**HAL** is a multi-disciplinary open access archive for the deposit and dissemination of scientific research documents, whether they are published or not. The documents may come from teaching and research institutions in France or abroad, or from public or private research centers.

L'archive ouverte pluridisciplinaire **HAL**, est destinée au dépôt et à la diffusion de documents scientifiques de niveau recherche, publiés ou non, émanant des établissements d'enseignement et de recherche français ou étrangers, des laboratoires publics ou privés.

# Observational evidence for active dust storms on Titan at equinox

S. Rodriguez<sup>1\*</sup>, S. Le Mouélic<sup>2</sup>, J. W. Barnes<sup>3</sup>, J. F. Kok<sup>4</sup>, S. C. R. Rafkin<sup>5</sup>, R. D. Lorenz<sup>6</sup>, B. Charnay<sup>7</sup>, J. Radebaugh<sup>8</sup>, C. Nartean<sup>1</sup>, T. Cornet<sup>9</sup>, O. Bourgeois<sup>2</sup>, A. Lucas<sup>10</sup>, P. Rannou<sup>10</sup>, C. A. Griffith<sup>11</sup>, A. Coustenis<sup>7</sup>, T. Appéré<sup>12</sup>, M. Hirtzig<sup>7,20</sup>, C. Sotin<sup>13</sup>, J. M. Soderblom<sup>14</sup>, R. H. Brown<sup>11</sup>, J. Bow<sup>3</sup>, G. Vixie<sup>3</sup>, L. Maltagliati<sup>1,21</sup>, S. Courrech du Pont<sup>15</sup>, R. Jaumann<sup>16</sup>, K. Stephan<sup>16</sup>, K. H. Baines<sup>17</sup>, B. J. Buratti<sup>13</sup>, R. N. Clark<sup>18</sup> and P. D. Nicholson<sup>19</sup>

**Saturn's moon Titan has a dense nitrogen-rich atmosphere, with methane as its primary volatile. Titan's atmosphere experiences an active chemistry that produces a haze of organic aerosols that settle to the surface and a dynamic climate in which hydrocarbons are cycled between clouds, rain and seas. Titan displays particularly energetic meteorology at equinox in equatorial regions, including sporadic and large methane storms. In 2009 and 2010, near Titan's northern spring equinox, the Cassini spacecraft observed three distinctive and short-lived spectral brightenings close to the equator. Here, we show from analyses of Cassini spectral data, radiative transfer modelling and atmospheric simulations that the brightenings originate in the atmosphere and are consistent with formation from dust storms composed of micrometre-sized solid organic particles mobilized from underlying dune fields. Although the Huygens lander found evidence that dust can be kicked up locally from Titan's surface, our findings suggest that dust can be suspended in Titan's atmosphere at much larger spatial scale. Mobilization of dust and injection into the atmosphere would require dry conditions and unusually strong near-surface winds (about five times more than estimated ambient winds). Such strong winds are expected to occur in downbursts during rare equinoctial methane storms—consistent with the timing of the observed brightenings. Our findings imply that Titan—like Earth and Mars—has an active dust cycle, which suggests that Titan's dune fields are actively evolving by aeolian processes.**

Along with Earth-based surveys, the close and frequent observations of Titan by the Cassini spacecraft, in orbit around Saturn since July 2004, allowed us to see down to Titan's surface and uncover evidence that the lowest part of its thick atmosphere experiences an exotic meteorological cycle analogous to Earth's hydrological cycle, involving methane evaporation, condensation into clouds<sup>1–5</sup> and rainfall<sup>1,5,6</sup>. Long-term monitoring campaigns have revealed that Titan's cloud coverage varies substantially with latitude and season<sup>1–4</sup>. General circulation models have suggested that the observed varying distribution of clouds is a natural consequence of the seasonally changing pattern of global atmospheric circulation<sup>1–4,7–11</sup>. This results in a net transport of methane from the tropics to the poles, drying the equatorial regions<sup>7–11</sup>. Titan's surface bears the marks of such climatic forcing through the presence of extensive and numerous liquid reservoirs and sustained cloud activity near the

poles<sup>1–4</sup>, and more arid conditions at the equator, with intense, but relatively scarce, meteorological activity<sup>3–5,12,13</sup> and widespread dune fields<sup>14,15</sup>.

Indeed, only a few tropospheric clouds have been observed in Titan's equatorial regions<sup>1–5,12,13</sup>. Very close to spring equinox (August 2009), with a more direct solar illumination of the equatorial regions, clouds occurred near the equator a little more frequently and appeared to grow in size and energy, counting three major events in April 2008, September 2010 and October 2010<sup>5,12</sup>. This increase in cloud activity indicates that a very active equinoctial meteorology occurs in the equatorial regions, confirming general circulation model predictions during this short time interval<sup>8–11</sup>. Here, we show new Cassini observations that illustrate the energetic meteorological conditions that prevail near Titan's equator during equinoxes and their possible impact on geomorphic processes.

<sup>1</sup>Institut de Physique du Globe de Paris, Sorbonne Paris Cité, Univ Paris Diderot, UMR 7154 CNRS, Paris, France. <sup>2</sup>Laboratoire de Planétologie et Géodynamique (LPGNantes), CNRS-UMR 6112, Université de Nantes, Nantes, France. <sup>3</sup>University of Idaho, Department of Physics, Moscow, ID, USA. <sup>4</sup>Department of Atmospheric and Oceanic Sciences, University of California, Los Angeles, CA, USA. <sup>5</sup>Planetary Atmospheres and Surfaces, Department of Space Studies, Southwest Research Institute, Boulder, CO, USA. <sup>6</sup>Johns Hopkins University Applied Physics Laboratory, Laurel, MD, USA. <sup>7</sup>LESIA, Observatoire de Paris, PSL-Research Univ., CNRS, Univ. Pierre et Marie Curie Paris 06, Sorbonne Univ., Univ. Paris-Diderot, Sorbonne Paris-Cité, Meudon, France. <sup>8</sup>Department of Geological Sciences, Brigham Young University, Provo, UT, USA. <sup>9</sup>European Space Agency (ESA), European Space Astronomy Centre (ESAC), Villanueva de la Canada, Spain. <sup>10</sup>Groupe de Spectroscopie Moléculaire et Atmosphérique, UMR CNRS 6089, Université de Reims, U.F.R. Sciences Exactes et Naturelles, Reims, France. <sup>11</sup>Department of Planetary Sciences, University of Arizona, Lunar and Planetary Laboratory, Tucson, AZ, USA. <sup>12</sup>Institut de Planétologie et d'Astrophysique de Grenoble, Université J. Fourier, CNRS/INSU, Grenoble, France. <sup>13</sup>California Institute of Technology/Jet Propulsion Laboratory, Pasadena, CA, USA. <sup>14</sup>Department of Earth, Atmospheric and Planetary Sciences, Massachusetts Institute of Technology, Cambridge, MA, USA. <sup>15</sup>Laboratoire Matière et Systèmes Complexes, Université Paris Diderot, Paris, France. <sup>16</sup>German Aerospace Centre (DLR), Institute of Planetary Research, Berlin, Germany. <sup>17</sup>Space Science and Engineering Center, University of Wisconsin, Madison, WI, USA. <sup>18</sup>Planetary Science Institute, Tucson, AZ, USA. <sup>19</sup>Department of Astronomy, Cornell University, Ithaca, NY, USA. <sup>20</sup>Present address: Fondation 'La main à la pâte', Montrouge, France. <sup>21</sup>Present address: Springer Nature, London, UK. \*e-mail: [rodriguez@ipgp.fr](mailto:rodriguez@ipgp.fr)

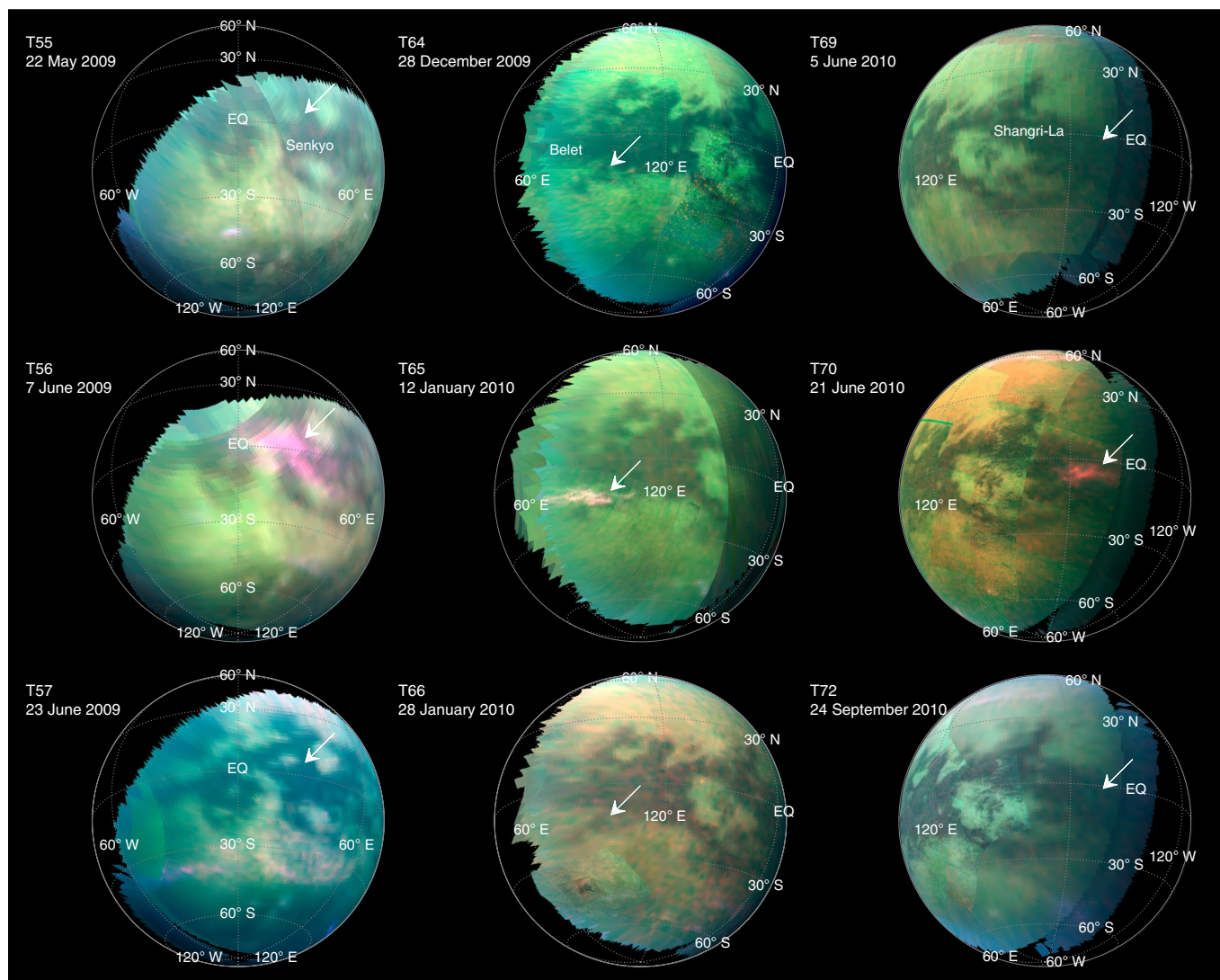


**Fig. 1 | VIMS colour composite maps of Titan's singular brightening events that occurred in June 2009 (T56 flyby), January 2010 (T65) and June 2010 (T70).** Each column presents a time series showing VIMS Titan images (using the same RGB (red, green, blue) coding, red being the average between  $5\mu\text{m}$  and  $5.07\mu\text{m}$ , green being  $2\mu\text{m}$  and blue being  $2.78\mu\text{m}$ ) acquired over the same area just before (top), during (middle) and immediately after (bottom) the brightening for each individual event. White arrows designate the location of the infrared brightenings, centred at  $-24^\circ\text{E}$  and  $-2^\circ\text{S}$  (T56),  $-96^\circ\text{E}$  and  $-14^\circ\text{S}$  (T65) and  $-175^\circ\text{W}$  and  $-5^\circ\text{S}$  (T70) and covering a large fraction of the Senkyo, Belet and Shangri-La sand seas, respectively (see also Supplementary Fig. 1b). EQ, equator.

### Infrared equatorial brightenings at equinox

We report here singular and transient changes on Titan in the form of diffuse bright spots of unusual infrared colour, which were detected by the Visual and Infrared Mapping Spectrometer (VIMS)<sup>16</sup> on board Cassini. Figures 1 and 2 show VIMS images and spectra of the only three events of this kind detected so far. They were observed during Titan flybys T56 (7 June 2009, Titan solar longitude  $L_s = 357.9^\circ$ ), T65 (12 January 2010,  $L_s = 5.3^\circ$ ) and T70 (21 June 2010,  $L_s = 10.7^\circ$ ), all near in time to Titan's northern spring equinox ( $L_s = 0^\circ$  by definition) (Supplementary Fig. 1a). These observations revealed an intense and short-lived infrared brightening of large regions usually dark, very close to the equator. These brightenings lasted at least 11 to 14 hours (time during which the brightened areas are visible from Cassini orbit), but no more than four to five terrestrial weeks (less than three Titan days), since they appeared in only one flyby, except for the T70 event, which was possibly still observable at T71 (7 July 2010). The three bright spots cover large areas, systematically over dune fields ( $\sim 420,000\text{ km}^2$  over Senkyo,  $\sim 250,000\text{ km}^2$  over Belet and

$\sim 180,000\text{ km}^2$  over Shangri-La for the T56, T65 and T70 events, respectively; Fig. 1 and Supplementary Fig. 1b), and present an elongated shape in the zonal direction. Spectrally, these bright spots are observed only at the centre and near wings of the infrared atmospheric windows, suggesting surface or very low atmospheric features (Supplementary Fig. 2). Their near-infrared ( $0.88\text{--}5.1\mu\text{m}$ ) spectra all present a pronounced positive slope (Fig. 2). They are brighter than the surrounding surface at wavelengths greater than  $1.6\mu\text{m}$ , particularly at  $5\mu\text{m}$ , and start dimming below  $1.6\mu\text{m}$ , fading almost totally at  $0.93\mu\text{m}$ , and thus are undetectable with the Imaging Science Subsystem cameras on board Cassini (Supplementary Fig. 3). Note that the affected areas have similar spectra before and after the ephemeral brightening events (Fig. 2). The spectral characteristics of these brightenings differ substantially from those of all known examples of surface and atmospheric brightenings, such as tropospheric clouds or deposition of frost onto the surface (Supplementary Fig. 3), which are bright and detectable in all near-infrared windows<sup>2,3,6</sup>, revealing a substantial difference in nature (composition and/or altitude) and origin.

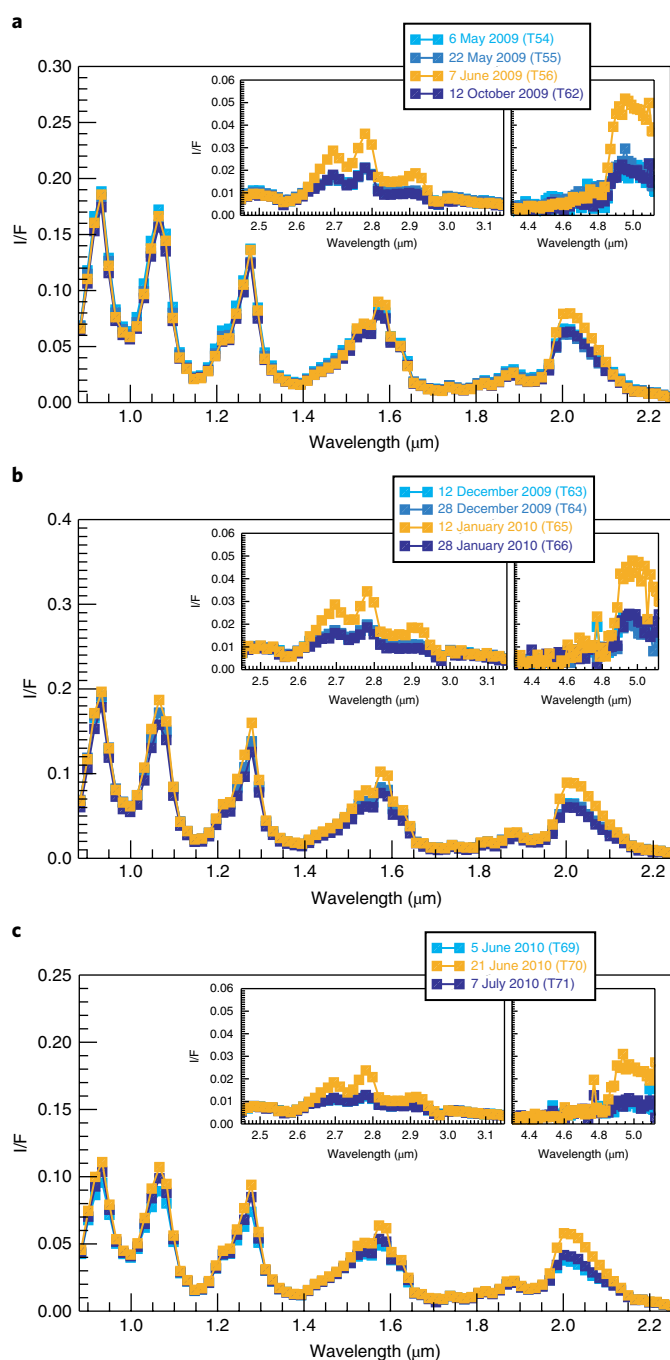


**Fig. 2 | VIMS infrared spectra of the brightening events that occurred at T56, T65 and T70 flybys. a–c.** The gold squares represent the infrared spectrum extracted from the brightest pixel in the central region of the brightening regions shown in Fig. 1 for T56 (a), T65 (b) and T70 (c). Each spectrum is compared with those extracted from the same location from flybys as close in time as possible, before and after the brightening event (blue-tone squares). The spectra are expressed in  $I/F$  where  $I$  is the observed specific intensity and  $\pi F$  is the incident solar flux.

### Evidence for large storms of organic dust

We investigate different possible explanations for these singular brightening events, considering both surface and atmospheric phenomena.

Given the particularly high brightness of these regions at  $5\ \mu\text{m}$ , we first examine the possibility of localized cryovolcanic hot spots. Considering that hypothetical eruptions on Titan are more likely effusive than explosive<sup>17</sup>, the sudden apparition of these bright (hot?)

spots over extensive areas is, however, hardly compatible with the slow outpouring and spreading of viscous lava flows. The timescale at which the T56, T65 and T70 events vanish is also difficult to reconcile with the timescale of cryolava cooling back to the average surface temperature of Titan, which has been calculated to be one to two orders of magnitude longer ( $\sim 100$  to  $1,000$  terrestrial days, depending on the lava composition<sup>18</sup>) than the observed durations. Finally, calculations of the thermal emission of a hot surface (with temperatures ranging from  $100\ \text{K}$  to  $250\ \text{K}$ ) show that no temperature can satisfactorily explain the spectral slope observed between  $1.6\ \mu\text{m}$  and  $5\ \mu\text{m}$  for the three events (Supplementary Fig. 5). Lava flows would also induce lasting surface changes, which are not observed.

Surface brightenings could be provoked by methane precipitation and subsequent freezing at the surface<sup>5,6</sup>. Such events have been reported by Imaging Science Subsystem and VIMS instruments in the wake of the September 2010 giant cloudburst<sup>6</sup> at roughly the same epoch and latitudes as the T56, T65 and T70 events. However, these precipitation-induced brightenings are characterized by an evolution timescale of several terrestrial months and a rise in flux in all atmospheric windows<sup>6</sup> (see an example in Supplementary Fig. 3). None of the T56, T65 and T70 bright spots match those characteristics.

Finally, we explore the possibility that these local rises in brightness may have an atmospheric origin. To that end, we apply a radiative transfer model that simulates the scattering and absorption of sunlight by Titan's atmosphere, producing synthetic spectra for comparison with the observations.

Our radiative transfer model is an updated version of the model presented in detail in Hirtzig et al.<sup>19</sup> (and references therein), using the same atmospheric databases (haze and gases) and a similar methodology to derive haze optical depth and surface albedo<sup>19</sup> (Supplementary Information). The main novelty concerns the possibility to simulate an additional 'cloud' layer composed of spherical particles in the lowest part of the atmosphere. This cloud is characterized by four parameters: top altitude, optical depth, particle effective radius and composition (either liquid methane or tholin-like organics analogous to Titan's airborne haze particles, presumably the main contributor to dune material composition<sup>15,19–24</sup>).

We first retrieved 'before' and 'after' surface albedos at the same location as the T56, T65 and T70 bright spots from flybys closely bracketing them in time (see Figs. 1 and 2). As the surface is clearly visible in those observations, we perform the radiative transfer calculations without the additional cloud layer. The striking similarity of the before and after surface albedos at all wavelengths (Supplementary Fig. 4) tells us that the brightening events have not substantially changed the properties of the surface.

These surface albedos were then used as inputs to model the event spectra extracted from the central and brightest pixel of the T56, T65 and T70 bright spots (Fig. 2). The surface-only model was unable to reproduce any of the event spectra, especially the high reflectance above  $1.6\ \mu\text{m}$  (Fig. 3). No enhancement in the local population of fractal aerosols or low-altitude mist, both too dark in the infrared<sup>19,25</sup>, especially at wavelengths greater than  $2\ \mu\text{m}$  (ref. 19), can better explain the observed spectra. We therefore searched for the best fits between observed and simulated spectra by adding a low-altitude cloud, for various opacities, particle sizes, top altitudes and compositions. The inversions have been performed by using a combination of genetic and Levenberg–Marquardt algorithms (Supplementary Information).

In all cases, the best fits to the observed spectra over the full VIMS infrared range are provided by the addition of a cloud of solid organic particles. Those tholin-like clouds are found to be optically thin, with opacity  $\sim 0.5$ , composed of small particles ( $\sim 5\ \mu\text{m}$  in diameter) and confined at low altitude, with a maximum top altitude of  $\sim 10$ – $14\ \text{km}$  (Fig. 3 and Supplementary Table 5).

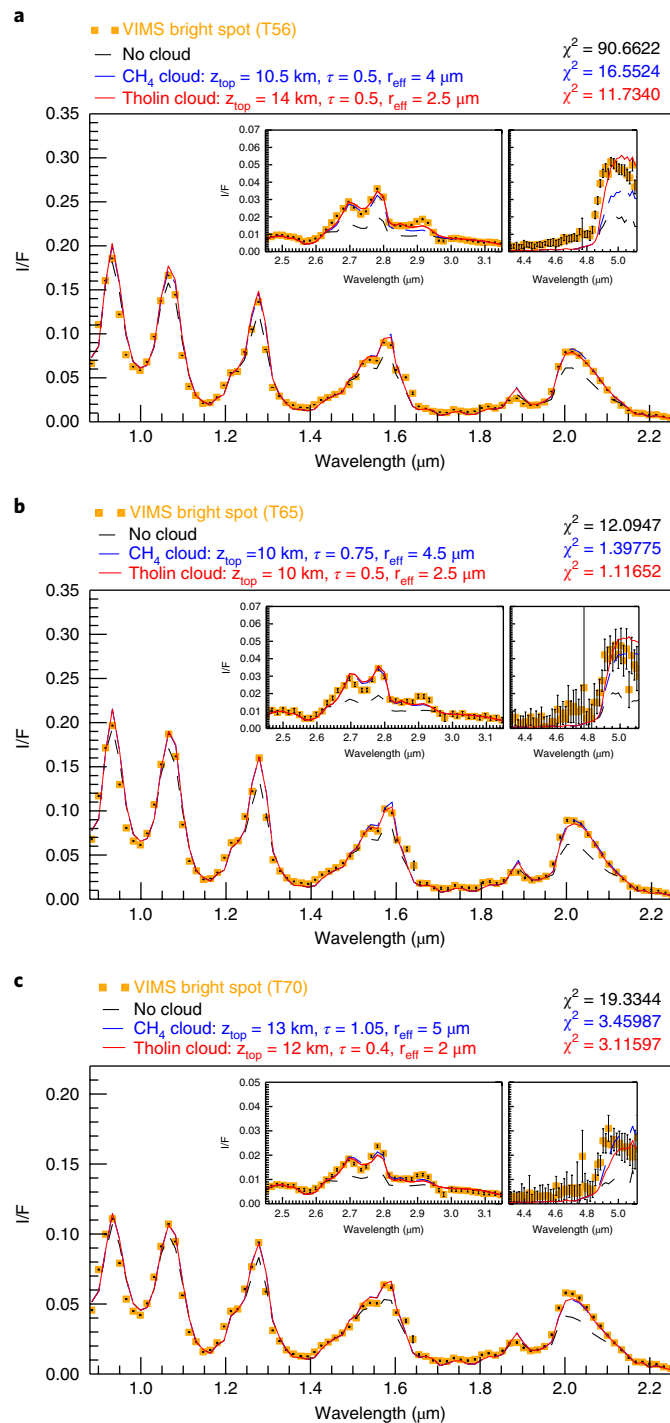


**Fig. 3 | Observed spectra of the brightest pixels compared with best-match calculated spectra. a–c.** The observed infrared spectra of the brightest pixels of the T56 (a), T65 (b) and T70 (c) bright spots are shown as gold squares (identical to the gold spectra shown in Fig. 2), along with their  $1\sigma$  error bars calculated from the VIMS signal-to-noise ratio. We modelled spectra with no cloud contribution (black dashed curves), with no satisfactory agreement with the observations. In all cases, the addition of a low-altitude cloud composed of solid organic particles (red curves) provides the best fits over the full VIMS wavelength range. Despite systematically poorer fits, best fits for liquid methane ( $\text{CH}_4$ ) clouds are also shown (blue dashed curves). Reduced  $\chi^2$  are indicated for the surface-only, liquid methane and solid organic cloud models, along with the best retrieved parameters for the two kinds of clouds (Supplementary Table 5). Simulated clouds are defined by four parameters: top altitude ( $z_{\text{top}}$ ), effective radius of the droplets ( $r_{\text{eff}}$ ), optical depth at  $2\ \mu\text{m}$  and composition (liquid methane or complex solid organics).

We cannot completely exclude liquid methane clouds, despite systematically poorer fits, on the sole basis of fitting statistics (Fig. 3 and Supplementary Table 5). However, the best retrieved parameters for methane clouds all point to unusually low top altitudes (10–13 km) and small droplet size ( $\sim 5\ \mu\text{m}$ ), casting some doubts on the possibility of their physical existence. Cloud simulations using the Titan Regional Atmospheric Modeling System (TRAMS)<sup>26,27</sup> were therefore conducted at the time and location of the observed brightenings, to further investigate both methane convective and stratiform clouds as possible explanations. The details and results of the cloud modelling studies are thoroughly discussed in the Supplementary Information. The radiative transfer modelling found that methane clouds, if real, should be restricted to altitudes below  $\sim 13\ \text{km}$  and probably lower (Fig. 3 and Supplementary Table 5). At the season and location where the brightenings are observed, thermodynamics suggest that any methane clouds with a base below this level would be necessarily convective in nature and would extend to much greater altitudes. Depending on the relative humidity of Titan's surface, the top altitude of such a convective cloud would reach at minimum 25 km. Moreover, we calculated the microphysical properties (droplet size distribution and number density) of such clouds with the TRAMS, still under the temperature and wind conditions at the equator and for the spring equinox, and we found that they are also completely inconsistent with the radiative transfer retrievals by several orders of magnitude. TRAMS simulations indeed lead to considerably optically thicker clouds than those possibly observed with VIMS and considered in this study. On their side, stratiform clouds below  $\sim 13\ \text{km}$  are not physically possible, given the thermodynamic sounding. Stratiform clouds above 13 km may be possible, but they would be shallow and also inconsistent with the physical properties of the retrieved clouds. For all these reasons, methane clouds, either convective or stratiform, as retrieved by the radiative transfer modelling, are simply unphysical and must be rejected.

Gathering together all of the observations, including locations (directly above giant sand seas), timing (close to spring equinox when the strongest winds are expected to episodically blow), spectral characteristics (pointing to solid organics equivalent to the material constituting the dunes) and cloud dynamics, we conclude that the best, and only remaining, explanation for these three bright spots may be short-lived dust storms composed of fine organic particles, smaller than sand-sized particles, lifted from the underlying dune fields.

### Implication for equatorial near-surface winds at equinoxes

At local scale, it has already been demonstrated not only that dust is likely to exist on the surface of Titan, but also that winds less than  $5\ \text{m s}^{-1}$  may lift it: the penetrometer of the Huygens probe, which landed near Titan's equator in 2005, indicated an uppermost thin (few millimetres) layer of soft/low-density material<sup>28</sup>, and optical measurements showed dust around the probe for 2–4 s after impact<sup>29</sup>. This dust was most possibly lifted by the turbulent aerodynamic wake of the probe<sup>29,30</sup>, which landed at  $5.4\ \text{m s}^{-1}$ . In our case, the possibility for large-scale storms of dust has more substantial implications for the atmospheric dynamics and sedimentology of the moon.

To investigate the possible onset of dust storms on Titan, we adapted models of sediment transport that were initially developed for Earth, Mars and Venus<sup>31–33</sup> to Titan's near-surface conditions. These models, based on semi-empirical or analytical calculations, allow us to predict the minimum friction velocity needed to initiate and sustain sediment transport (Fig. 4 and Supplementary Information).

Dust can be emitted through three primary processes<sup>34</sup>: (1) direct aerodynamic lifting, (2) indirect ejection from the surface by impacts of saltating sand particles or (3) lifting of sand-sized aggregates of dust particles that fragment on impact on the surface. Our

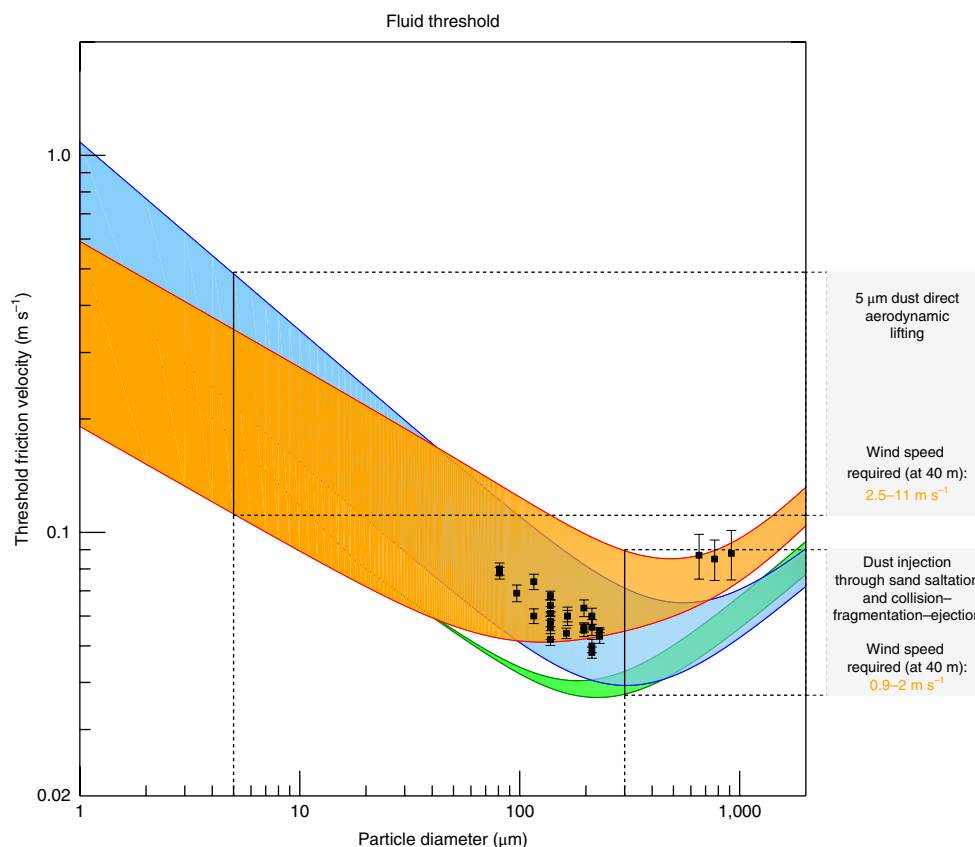


**Fig. 4 | Transport thresholds on Titan.** Intervals of friction velocity at the fluid threshold computed from formulae given in ref.<sup>31</sup> (green area), ref.<sup>32</sup> (blue area) and ref.<sup>33</sup> (orange area) for a range of possible mass densities (800–1,200 kg m<sup>-3</sup>) and interparticle forces ( $\gamma=1\text{--}5\times 10^{-4}$  N m<sup>-1</sup>) for Titan's surface material<sup>32</sup> (see Supplementary Table 6). The calculated threshold curves are in very good agreement with recent wind-tunnel measurements under Titan's atmospheric and sedimentary conditions<sup>40</sup> (black squares with s.d. error bars). The range of needed near-surface wind speeds is given for 5  $\mu\text{m}$  dust direct aerodynamic lifting and for dust injection through saltation and collision-fragmentation-ejection processes, respectively.

radiative transfer modelling points to particles in suspension with a diameter of  $\sim 5\mu\text{m}$ . Aerodynamic lifting of such small particles, which experience large cohesive forces, requires minimum friction velocities as high as  $0.1\text{--}0.5\text{ m s}^{-1}$  (Fig. 4). Using the classical von Kármán logarithmic wind velocity profile with a rugosity length of 5 mm, those friction velocities correspond to a wind blowing at  $\sim 2.5\text{--}11\text{ m s}^{-1}$  at 40 m altitude. Dust emission through saltation of sand particles (with an optimal size of  $300\mu\text{m}$ ) would have a lower threshold friction velocity for lifting ( $\sim 0.06\text{ m s}^{-1}$ ) than that for dust (Fig. 4), which would require wind speed of  $\sim 1.4\text{ m s}^{-1}$  at 40 m altitude. However, compared with Earth and Mars, the lower gravity and higher fluid density on Titan substantially reduces the energy with which saltating particles impact the surface<sup>34</sup>. This implies that dust emission through saltator bombardment may be less efficient than it is on Earth and Mars (Supplementary Fig. 10). Dust could also be emitted through the formation<sup>35</sup>, lifting and fragmentation at impact of sand-sized aggregates of dust. Owing to their lower density, such aggregates could present a threshold for lifting slightly below  $1.4\text{ m s}^{-1}$  and be more easily lifted than dust and sand particles<sup>34</sup>. Dust emission through this process would not necessarily involve active sand transport, an effect that has been observed directly on Mars<sup>36</sup>. In any case, micrometre-sized dust emission is systematically accompanied by the mobilization of larger particles, more easily unstuck from the surface (Fig. 4). Since larger particles have higher fall velocity and will settle down rapidly, they generally stay confined close to the surface, while smaller particles can rise to higher altitudes and remain suspended for much longer times, generating the observed dust cloud. This is what can be observed

in terrestrial and Martian dust storms and can explain why the dust clouds we report here are dominated by the infrared signature of micrometre-sized particles.

Regardless of the process, dust injection into the atmosphere requires near-surface winds much stronger than the ambient averaged winds predicted to blow during equinoxes (maximum of  $\sim 0.3\text{ m s}^{-1}$  at 40 m altitude; for example, ref.<sup>10</sup>). Only gusts, either appearing when considering wind statistics at high temporal frequency (that is, capturing the turbulence associated with the equinoctial passage of the intertropical convergence zone<sup>37</sup>) or produced ahead of rare, but large, methane storms, as simulated in mesoscale methane cloud models<sup>38,39</sup>, can exceed  $1\text{ m s}^{-1}$  at 40 m altitude, and even reach  $10\text{ m s}^{-1}$  for a few hours for the methane storms<sup>38,39</sup>. In both cases, gusts have the highest probability of occurring during equinox in the equatorial regions, precisely when and where we possibly observe the dust storms. A few large equatorial storms have been observed very close to the equinox<sup>5,12</sup> (Supplementary Fig. 1a). The most energetic of these may constitute the best, and timely, candidates for generating surface winds strong enough to inject organic dust into Titan's air (this mechanism would thus be analogous to Earth's 'haboobs'). Their uncommonness may further explain the rareness of dust storm detections by Cassini. Such equatorial storms are also thought to sustain active sediment transport over the dunes and control their growth and orientation<sup>38</sup>.

No equatorial methane storms have yet been detected preceding closely any of the T56, T65 and T70 events. However, given the frequency of Cassini flybys of Titan (one per month on average) and the relatively short lifetime of methane storms (only a few to a few tens of

hours), it is likely that those precursors have been missed and that we were able to see only the succeeding, and more persistent, dust cloud. In a similar manner, no dust storms have been seen by Cassini after the gigantic methane storms observed in Titan's equatorial regions in October 2010<sup>5</sup>, but the fact that Cassini flew back by Titan only four months later may explain that, in that case, no dust storm could have been triggered or that we may have missed this event, if any.

The requirement of strong near-surface winds implies that dust lifting can be accompanied by saltation of the underlying dune sand. This constitutes additional clues for sand-saltating winds in currently active dune fields. This may occur only at equinoxes, every 14.7 terrestrial years. Besides Earth and Mars, Titan would thus be the only other body in the Solar System where dust storms and aeolian activity over dune fields have been observed, indicating the complexity of the atmospheric dynamics and atmosphere–surface interactions at play on Saturn's largest moon. The dust storms may also indicate ongoing participation of dust in Titan's global organic cycle<sup>35</sup>.

### Online content

Any methods, additional references, Nature Research reporting summaries, source data, statements of data availability and associated accession codes are available at <https://doi.org/10.1038/s41561-018-0233-2>.

Received: 22 October 2017; Accepted: 20 August 2018;

Published online: 24 September 2018

### References

- Turtle, E. P. et al. Cassini imaging of Titan's high-latitude lakes, clouds, and south-polar surface changes. *Geophys. Res. Lett.* **36**, L2204 (2009).
- Rodriguez, S. et al. Global circulation as the main source of cloud activity on Titan. *Nature* **459**, 678–682 (2009).
- Rodriguez, S. et al. Titan's cloud seasonal activity from winter to spring with Cassini/VIMS. *Icarus* **216**, 89–110 (2011).
- Turtle, E. P. et al. Seasonal changes in Titan's meteorology. *Geophys. Res. Lett.* **38**, L03203 (2011).
- Turtle, E. P. et al. Rapid and extensive surface changes near Titan's equator: evidence of April showers. *Science* **331**, 1414–1417 (2011).
- Barnes, J. W. et al. Precipitation-induced surface brightenings seen on Titan by Cassini VIMS and ISS. *Planet. Sci.* **2**, 1 (2013).
- Rannou, P., Montmessin, F., Hourdin, F. & Lebonnois, S. The latitudinal distribution of clouds on Titan. *Science* **311**, 201–205 (2006).
- Mitchell, J. L. The drying of Titan's dunes: Titan's methane hydrology and its impact on atmospheric circulation. *J. Geophys. Res. Planets* **113**, E08015 (2008).
- Schneider, T., Graves, S. D. B., Schaller, E. L. & Brown, M. E. Polar methane accumulation and rainstorms on Titan from simulations of the methane cycle. *Nature* **481**, 58–61 (2012).
- Lora, J. M., Lunine, J. I. & Russell, J. L. GCM simulations of Titan's middle and lower atmosphere and comparison to observations. *Icarus* **250**, 516–528 (2015).
- Mitchell, J. L. & Lora, J. M. The climate of Titan. *Annu. Rev. Earth Planet. Sci.* **44**, 353–380 (2016).
- Schaller, E. L., Roe, H. G., Schneider, T. & Brown, M. E. Storms in the tropics of Titan. *Nature* **460**, 873–875 (2009).
- Griffith, C. A. et al. Characterization of clouds in Titan's tropical atmosphere. *Astrophys. J.* **702**, L105–L109 (2009).
- Lorenz, R. D. et al. The sand seas of Titan: Cassini RADAR observations of longitudinal dunes. *Science* **312**, 724–727 (2006).
- Rodriguez, S. et al. Global mapping and characterization of Titan's dune fields with Cassini: correlation between RADAR and VIMS observations. *Icarus* **230**, 168–179 (2014).
- Brown, R. H. et al. The Cassini Visual and Infrared Mapping Spectrometer investigation. *Space Sci. Rev.* **115**, 111–168 (2004).
- Lorenz, R. D. Pillow lava on Titan: expectations and constraints on cryovolcanic processes. *Planet. Space Sci.* **44**, 1021–1028 (1996).
- Davies, A. G. et al. Atmospheric control of the cooling rate of impact melts and cryolavas on Titan's surface. *Icarus* **208**, 887–895 (2010).
- Hirtzig, M. et al. Titan's surface and atmosphere from Cassini/VIMS data with updated methane opacity. *Icarus* **226**, 470–486 (2013).
- Soderblom, L. A. et al. Correlations between Cassini VIMS spectra and RADAR SAR images: implications for Titan's surface composition and the character of the Huygens probe landing site. *Planet. Space Sci.* **55**, 2025–2036 (2007).
- Barnes, J. W. et al. Spectroscopy, morphometry, and photogrammetry of Titan's dune fields from Cassini/VIMS. *Icarus* **195**, 400–414 (2008).
- Clark, R. N. et al. Detection and mapping of hydrocarbon deposits on Titan. *J. Geophys. Res. Planets* **115**, E10005 (2010).
- Le Gall, A. et al. Cassini SAR, radiometry, scatterometry and altimetry observations of Titan's dune fields. *Icarus* **213**, 608–624 (2011).
- Bonnefoy, L. E. et al. Compositional and spatial variations in Titan dune and interdune regions from Cassini VIMS and RADAR. *Icarus* **270**, 222–237 (2016).
- Tomasko, M. G. et al. A model of Titan's aerosols based on measurements made inside the atmosphere. *Planet. Space Sci.* **56**, 669–707 (2008).
- Barth, E. L. & Rafkin, S. C. R. TRAMS: a new dynamic cloud model for Titan's methane clouds. *Geophys. Res. Lett.* **34**, L03203 (2007).
- Barth, E. L. & Rafkin, S. C. R. Convective cloud heights as a diagnostic for methane environment on Titan. *Icarus* **206**, 467–484 (2010).
- Atkinson, K. R. et al. Penetrometry of granular and moist planetary surface materials: application to the Huygens landing site on Titan. *Icarus* **210**, 843–851 (2010).
- Schroeder, S. E., Karkoschka, E. & Lorenz, R. D. Bouncing on Titan: motion of the Huygens probe in the seconds after landing. *Planet. Space Sci.* **73**, 327–340 (2012).
- Lorenz, R. D. Wake-induced dust cloud formation following impact of planetary landers. *Icarus* **101**, 165–167 (1993).
- Greeley, R. & Iversen, J. D. *Wind as a Geological Process on Earth, Mars, Venus, and Titan* (Cambridge Univ. Press, Cambridge, 1985).
- Shao, Y. P. & Lu, H. A simple expression for wind erosion threshold friction velocity. *J. Geophys. Res. Atmos.* **105**, 22437–22443 (2000).
- Claudin, P. & Andreotti, B. A scaling law for aeolian dunes on Mars, Venus, Earth, and for subaqueous ripples. *Earth Planet. Sci. Lett.* **252**, 30–44 (2006).
- Kok, J. F., Parteli, E. J. R., Michaels, T. I. & Karam, D. B. The physics of wind-blown sand and dust. *Rep. Prog. Phys.* **75**, 106901 (2012).
- Barnes, J. W. et al. Production and global transport of Titan's sand particles. *Planet. Sci.* **4**, 1 (2015).
- Sullivan, R. et al. Wind-driven particle mobility on Mars: insights from Mars Exploration Rover observations at 'El Dorado' and surroundings at Gusev Crater. *J. Geophys. Res. Planets* **113**, E06S07 (2008).
- Tokano, T. Relevance of fast westerlies at equinox for eastward elongation of Titan's dunes. *Aeolian Res.* **2**, 113–127 (2010).
- Charnay, B. et al. Methane storms as a driver of Titan's dune orientation. *Nature Geosci.* **8**, 362–366 (2015).
- Rafkin, S. C. R. & Barth, E. L. Environmental control of deep convective clouds on Titan: the combined effect of CAPE and wind shear on storm dynamics, morphology, and lifetime. *J. Geophys. Res. Planets* **120**, 739–759 (2015).
- Burr, D. M. et al. Higher-than-predicted saltation threshold wind speeds on Titan. *Nature* **517**, 60–63 (2015).

### Acknowledgements

We thank P. Claudin and B. Andreotti for discussions, especially regarding thresholds and modes of sediment transport. We are also grateful to the Cassini/VIMS team for the calibration and planning of the data. We acknowledge financial support from the UnivEarthS LabEx programme of Sorbonne Paris Cité (ANR-10-LABX-0023 and ANR-11-IDEX-0005-02), the French National Research Agency (ANR-APOSTIC-11-BS56-002 and ANR-12-BS05-001-03/EXO-DUNES) and the CNES. This study was partly supported by the Institut Universitaire de France. T.C. was funded by the ESA Research Fellowship Programme in Space Sciences. Part of this work has been performed at the Jet Propulsion Laboratory, California Institute of Technology, under contract with NASA.

### Author contributions

S.R., S.L.M., J.W.B., J.B. and G.V. discovered the brightening spots in the VIMS dataset and proposed the dust storm hypothesis. S.R., T.A., M.H., L.M., P.R., C.A.G. and A.C. developed, adapted and ran the radiative transfer model and designed the inversion scheme, including a low atmospheric layer of suspended particles. B.C., J.F.K., R.D.L., J.R., C.N. and S.C.P. helped with the wind and sediment transport calculations. J.F.K., C.N., T.C., O.B. and A.L. participated in the discussion of the geological implications of dust storm occurrence in Titan's atmosphere. C.S., R.H.B., K.H.B., B.J.B., R.N.C. and P.D.N. designed the planning of VIMS observations. S.R. drafted the manuscript with contributions from all authors.

### Competing interests

The authors declare no competing interests.

### Additional information

**Supplementary information** is available for this paper at <https://doi.org/10.1038/s41561-018-0233-2>.

**Reprints and permissions information** is available at [www.nature.com/reprints](http://www.nature.com/reprints).

**Correspondence and requests for materials** should be addressed to S.R.

**Publisher's note:** Springer Nature remains neutral with regard to jurisdictional claims in published maps and institutional affiliations.

**Methods**

Details about the methods employed in this paper can be found in the Supplementary Information.

**Code availability.** The radiative transfer codes used to analyse Titan's spectra can be accessed from the corresponding author upon request.

**Data availability**

VIMS data are available via NASA's Planetary Data System (PDS): [http://pds-atmospheres.nmsu.edu/data\\_and\\_services/atmospheres\\_data/Cassini/vims.html](http://pds-atmospheres.nmsu.edu/data_and_services/atmospheres_data/Cassini/vims.html). The data that support the analysis and plots within this paper and other findings of this study are available from the corresponding author upon request.